REPORT DOCUMENTATION PAGE

AFOSR-TR-95 0618

1. AGENCY USE ONLY (Leave blank)	2. REPORT DATE	3. REPORT TYPE AND DATES COVERED
	October 1994	Final Technical Report 4/92 - 10/94

4. TITLE AND SUBTITLE

(U) A Study of Mixing and Combustion in the Presence of a Strong Streamwise Vorticity

5. FUNDING NUMBERS

PE - 61102F
PR - 2308
SA - BS
G-F49620-92-J-0224

6. AUTHOR(S)

V. M. Belovich, M. Samimy, and M. F. Reeder

7. PERFORMING ORGANIZATION NAME(S) AND ADDRESS(ES)

The Ohio State University
Department of Mechanical Engineering
Columbus, Ohio 43210

8. PERFORMING ORGANIZATION REPORT NUMBER

MEMS-94-102

9. SPONSORING/MONITORING AGENCY NAME(S) AND ADDRESS(ES)

AFOSR/NA
110 Duncan Avenue, Suite B115
Bolling AFB DC 20332-0001

10. SPONSORING/MONITORING AGENCY REPORT NUMBER

SUPPLEMENTARY NOTES

DISTRIBUTION/AVAILABILITY STATEMENT

Approved for public release;
distribution is unlimited

12b. DISTRIBUTION CODE

ABSTRACT (*Maximum 200 words*)

An experimental investigation was undertaken to study the mixing process in a coaxial jet with an inner lobed mixer nozzle. Seven different inner jet nozzle geometries and also three different velocity ratios were explored. Flow visualizations using a passive scalar were performed using a laser sheet from a Nd:YAG laser as the light source. The laser has a 9 nsec pulse duration which effectively freezes the flow. Instantaneous cross sectional images were taken at various distances downstream as well as streamwise views. Quantitative information on the mixing was obtained by processing sets of images. The effects of various parameters such as the interfacial area increase due to the lobed nozzle geometry, the strength of streamwise vortices, and the large scale structures on the mixing process are evaluated and discussed. The results showed highly enhanced mixing as the strength of the streamwise vortices increased. The results also indicated that the presence of large scale structures due to the Kelvin-Helmholtz instabilities and their interaction with streamwise vortices generated by the lobes are crucial for enhanced mixing. The fraction of mixing enhancement due to streamwise vorticity (relative to mixing enhancement due to increased interfacial contact area) was found to increase as velocity ratio increased. In addition, this fraction increased with downstream distance.

14. SUBJECT TERMS	15. NUMBER OF PAGES
Mixing Enhancement, Streamwise Vorticity, Lobed Mixer, Flow Visualizations, Feed Back Loop, Unsteady Mixing	36
	16. PRICE CODE

17. SECURITY CLASSIFICATION OF REPORT	18. SECURITY CLASSIFICATION OF THIS PAGE	19. SECURITY CLASSIFICATION OF ABSTRACT	20. LIMITATION OF ABSTRACT
Unclassified	Unclassified	Unclassified	Unlimited

Dual Stream Axisymmetric Mixing in the Presence of Axial Vorticity

V. M. Belovich[1], M. Samimy[2], and M. F. Reeder[3]
Department of Mechanical Engineering
The Ohio State University
Columbus, OH 43210

Final Technical Report

for

The Air Force Office of Scientific Research
Grant F49620-92-J-0224

September 1994

[1] Graduate Student, Palace Knight Fellow
[2] Principal Investigator, Professor
[3] Graduate Student, NASA GSRP Fellow

ACKNOWLEDGEMENTS

The authors would like to thank Dr. W.M. Roquemore for many helpful discussions. The authors would also like to thank the support staff of AARL for their cooperation. The first author is supported by the Air Force Senior Knight Program, with Dr. W.M. Roquemore serving as mentor. The third author is supported by the NASA Graduate Student Researcher Program.

ABSTRACT

An experimental investigation was undertaken to study the mixing process in a coaxial jet where the inner nozzle is a lobed mixer. Seven different inner jet nozzle geometries were explored: a baseline circular jet, three different six-lobed nozzles, and three different four-lobed nozzles. Also, three different velocity ratios of 3:1, 1:1 and 1:3 (inner:outer) were examined. Flow visualizations using a passive scalar (tobacco smoke) were performed using a laser sheet from a Nd:YAG laser as the light source. The laser has a 9 nsec pulse duration which effectively freezes the flow. Instantaneous cross sectional images were taken at various distances downstream as well as streamwise views. Quantitative information on the mixing was obtained by processing sets of images. The effects of various parameters such as the interfacial area increase due to the lobed nozzle geometry, the strength of streamwise vortices, and the large scale structures on the mixing process are evaluated and discussed. The results showed highly enhanced mixing as the strength of the streamwise vortices increased. The results also indicated that the presence of large scale structures due to the Kelvin-Helmholtz instabilities and their interaction with streamwise vortices generated by the lobes are crucial for enhanced mixing. The fraction of mixing enhancement due to streamwise vorticity (relative to mixing enhancement due to increased interfacial contact area) was found to increase as velocity ratio increased. In addition, this fraction increased with downstream distance.

PERSONNEL

Two graduate students, Vincent M. Belovich and Mark F. Reeder, worked on the project. Vincent Belovich was supported by the Air Force Palace Knight Program. The project was a major part of his Ph.D. dissertation research. Mark Reeder, who helped Vincent Belovich occasionally on this project, was a fellow of the NASA Graduate Student Researchers Program.

PUBLICATIONS

1. Journal Articles

Belovich, V. M., Samimy M., and Reeder, M.F., "Dual Stream Axisymmetric Mixing in Presence of Axial Vorticity," submitted to Journal of Propulsion and Power, August, 1994.

2. Conference Papers

Belovich, V. M., Samimy M., and Reeder, M.F., "Dual Stream Axisymmetric Mixing in Presence of Axial Vorticity," AIAA-94-3084, June, 1994.

PRESENTATIONS

1. "Dual Stream Axisymmetric Mixing in Presence of Axial Vorticity," AFOSR Propulsion Contractors Meeting, Atlantic City, New Jersey, June, 1993.

2. "Dual Stream Axisymmetric Mixing in Presence of Axial Vorticity," 30th Joint Propulsion Meeting, Indianapolis, June, 1994.

INTERACTION RELATED TO THE RESEARCH

The project started as a joint effort between the Fuels and Lubrication Branch of Wright Laboratories under Dr. M. L. Roquemore and the Department of Mechanical Engineering at The Ohio State University under Professor M. Samimy. Initially, Dr. G. J. Sturgess of Pratt and Whitney provided guidance from an industrial perspective. The original idea was to design a bench-top type experimental facility that could be used for cold flow experiments at The Ohio State University and combustion experiments at Wright Laboratories. Unfortunately, after about a year into the project, designing such a test rig was proved to be not feasible. Therefore, the test rig was designed to only conduct cold flow experiments at The Ohio State University. However, interactions between two laboratories are on going.

INVENTIONS

There was no invention on this project.

I. INTRODUCTION AND BACKGROUND

Mixing is an important phenomenon in combustion processes from low-speed systems such as coal-fired boilers, oil and gas fired furnaces, and gas turbine engines, to high speed systems such as scramjets and flows through the exhaust nozzles of supersonic aircraft. A critical technical problem to be solved in many of these applications is the mixing between two gaseous streams. How quickly and how well a fuel and oxidant can be mixed will have a major influence on the combustion efficiency, heat release rate, pollutant formation, combustor size, and many other critical parameters. Vorticity dynamics greatly impact the mixing process. The streamwise vortices generated in a flow, in addition to the spanwise (in planar shear layers) or ring type (in axisymmetric shear layers) vortex roll up process have been found to mix fluid streams quickly and efficiently. Generating these vortical structures using a lobed mixer and investigating the nature of these structures and their mixing enhancement capabilities are the subject of the present study.

The lobed mixer produces streamwise vortices (e.g., Paterson,[1,2] Povinelli et al.[3]) on the order of the nozzle dimensions. These relatively large scale streamwise vortices aid the mixing process by entraining additional fluid from the secondary stream into the mixing layer, and conversely, sweeping the primary flow into the secondary stream.

Most of the early studies of lobed mixers (Frost,[4] Anderson et al.,[5] Birch et al.,[6] Blackmore and Thompson,[7] Crouch et al.,[8] Head et al.,[9] Kozlowski and Kraft,[10] Kuchar and Chamberlain,[11] Shumpert,[12] Packman et al.,[13] Povinelli et al.,[3] Povinelli and Anderson[14]) were greatly influenced by the gas turbine industry, as many of the test configurations were scale models of turbo-fan engine exhaust sections. The geometry consisted of a central solid body around which flowed the hot core fluid with the bypass air surrounding the core. The lobed mixer was an axisymmetric shape separating the two fluid streams. Among the significant findings of these studies was that lobed mixers generate streamwise vorticity more efficiently (i.e., with less pressure drop) than the conventional methods, and thus provide an engine performance improvement. Another important benefit of lobed mixers is that their improved entrainment reduces the velocity of the high speed exhaust gases, thereby reducing noise. Other findings include: scalloping the lobes aids in mixing, and lobe penetration in the fluid streams has the most significant effect on mixing effectiveness, as long as the flow does not separate. Separation increases the pressure losses and decreases mixing effectiveness.

Paterson[1,2] studied subsonic flow issuing from a lobed nozzle for both cold and heated flows. Detailed pressure and temperature data were taken, as well as three dimensional laser Doppler velocimetry (LDV) measurements. Paterson found that large scale secondary flows, set up by the nozzle, produced streamwise vortices of low intensity with a length scale on the order of the nozzle radius. Also, a horseshoe vortex on the order of the lobe half width was found to exist in the lobe troughs. The contribution to the overall mixing process of each was not clear, but the secondary flow vortices were expected to be dominant because of their much greater size. The lobed mixer was found to rapidly mix flows at large scale.

Much of the later work on lobed mixers concentrated on understanding the underlying physics of the lobed mixing process by using a two dimensional lobed mixer, which is essentially a corrugated plate. Werle et al.,[15] found that the vortex formation process was an inviscid one. Also, the mixing process was proposed to take place in three basic steps: the vortices form, intensify, and then rapidly break down into small scale turbulence. In effect, the lobed mixer was thought to act as a 'fluid stirrer' initially to mix the flow, until the rapid breakdown of the vortices produces small scale, and possibly, molecular mixing.

Other studies during the last ten years or so tested the performance of a lobed mixer in applications such as in ejectors (Presz et al.,[16] Skebe et al.,[17] Malecki et al.[18]) in supersonic flow (Tillman et al.,[19] Malecki et al.,[18]) and in combustion (McVey,[20] McVey and Kennedy[21]).

Eckerle et al.,[22] used two component LDV to study mixing downstream of a lobed mixer at two velocity ratios. They determined that the breakdown of the large scale vortices and the accompanying increase in turbulent mixing, are important parts of the mixing process. It was also shown that this vortex breakdown occurs further upstream for a velocity ratio of 2:1 than for 1:1.

Barber et al.,[23] studied three different two dimensional lobed mixers both analytically and experimentally. Performing a one dimensional inviscid analysis to predict lobe circulation and geometrical scaling relations produced results in reasonable agreement with their data, further emphasizing the inviscid nature of the overall large scale mixing process. Circulation was found to scale well according to the following relation,

$$\Gamma \propto C U_{ref} \frac{h^2}{L}, \tag{1}$$

where C is a constant, U_{ref} is the mean freestream velocity, h is the lobe height and L is the length of the lobe. For a straight contour (in the axial direction) lobe, the ramp angle can be found by

$$\alpha = \tan^{-1}\left(\frac{h}{L}\right) \tag{2}$$

Thus, circulation is essentially proportional to ramp angle. One of the conclusions of the study was that lobed mixers with parallel side walls produce higher streamwise circulation than lobes with sinusoidal or triangular shapes. The close proximity of the walls in the lobe peak region for the latter shapes creates thicker boundary layers that reduce the effective lobe height, and therefore reduce circulation. The lobes for the nozzles of the present study have a radial geometry. That is, the sides of the lobes are directed along radii, and thus the lobe width increases away from the axis centerline.

Mixing downstream of a lobed mixer is controlled by three primary elements. The first element is the increased interfacial area between the two fluid streams because of the convoluted trailing edge of the nozzle. The second is the streamwise vorticity generated due to the alternate inwardly and outwardly angled flow paths of the air through the nozzle. The third is the Brown-Roshko type structures which are generated in any free shear layer with velocity gradients across the layer, due to the Kelvin-Helmholtz instabilities. Manning[24] attempted to separate the effects of these three mechanisms in two dimensional water tunnel experiments. He studied a flat plate, for use as a baseline case, and two different lobed mixers--one of which had a convoluted, yet straight (i.e., no ramp angle) extension section to damp the streamwise vorticity. It was shown that the mixing performance of the lobed mixer exceeds the performance of the convoluted plate by an amount that increases with velocity ratio. Also, at velocity ratios close to 1, the increased mixing is due mainly to the increased contact area, whereas the streamwise vorticity has the larger role at a velocity ratio of 2. Manning's work and the work of his colleagues are summarized in Elliott et al.[25]

A very detailed and systematic study by McCormick[26] revealed several more details of the flow patterns downstream of a lobed mixer. Extensive flow visualizations for laminar and turbulent air flow and three dimensional velocity measurements taken with a hot-wire, showed that the interaction of Kelvin-Helmholtz (normal) vortices with the streamwise vortices produces the high levels of mixing. The streamwise vortices pinch off the normal vortices, thus enhancing the stirring effect in the flow. This pinching causes the normal vortices to merge within 1.5 lobe heights downstream, where they were observed to break down shortly thereafter, leading to intense turbulent mixing. Another interesting observation by McCormick is that the scale of the normal vortices shed from the lobed mixer is about 1/4 that shed from a planar baseline case. From this McCormick and Bennett[27] infer that the lobed mixer introduces smaller scales into a flow sooner, which may enhance molecular mixing.

Presz et al.,[28] studied axisymmetric lobed mixers used in ejector applications. They found that an aggressively designed mixer, having ramp angles of 45° inward, 30° outward and scalloped lobes, produced pumping performance approaching ideal values. Scalloping the lobes has also been used before with success (Kozlowski and Kraft[10]). The study of Presz et al. is significant to the present work because it is a return to the original axisymmetric designs of the 1970s and early 1980s, but with a significant difference. The difference is that the earlier work used a center body to represent the core/shaft of the jet engine. The center body created an inner annular flow (hot core flow), surrounded by the lobed mixer nozzle which separated it from the outer annular flow (bypass, or fan flow). In effect, two annular flows were being mixed.

As in the experiments of Presz et al., the present study uses the lobed mixer as a central round jet, which mixes with an outer (annular) flow. By varying the velocity ratio of inner flow to outer flow as well as the nozzle geometry, the three primary elements which affect mixing with lobed nozzles were studied. The present study parallels in many ways that of Manning.[24] However, that work was concerned exclusively with two dimensional mixing layers and low Reynolds number.

II. EXPERIMENTAL FACILITY AND TECHNIQUES

A. Facility

The experiments for this work were conducted at the Aeronautical and Astronautical Research Laboratory at the Ohio State University. The air supply for the tests is provided by two four-stage compressors and is stored in two tanks of 42.5 m^3 (1500 ft^3) volume at pressures up to 16.9 MPa (2450 psi). The air is throttled through two valves, plumbed through two inch steel pipe and separated into two branches through a Tee section. One branch supplies the primary (central) flow, the other supplies the secondary (outer) flow. Downstream of the Tee are two ball valves used for regulating the inner and outer flows to the test sections. The flow rates are metered using Dwyer model DS-200 flow sensors which are averaging pitot probe devices and require the measurement of differential and static pressures. The differential pressures are measured using a Dwyer model 422-23 incline manometer for the central flow and a Dwyer model 1230-16 U-tube manometer for the outer flow. At high flow rates, a mercury manometer is used for the outer flow. Calibrated gauges are used for the static pressure measurements.

Figure 1 shows a schematic of the settling chamber and the contraction section. Primary flow enters through a single central tube, while the secondary flow enters through two separate bottom inlets. The secondary air is forced to exit radially into the settling chamber through a wire screen at each inlet. The flow then passes through a 25% open perforated plate and two 51% open perforated plates to reduce the turbulence level and flatten the velocity profiles. The contraction section is smoothly contoured (5th order polynomial) with a 7.44 to 1 area ratio and an exit diameter of 63.5 mm (2.5 in.). The end piece of the outer nozzle is two inches long and constructed out of plexiglas. The system was designed to allow for a wide range of primary and secondary flow rates and velocity ratios. Velocities at the exit up to 120 m/sec can easily be maintained in either the primary or secondary flows.

Tobacco smoke was injected upstream of the stagnation chamber into the primary stream. The smoke patterns were illuminated using a Quanta Ray GCR-4 frequency doubled (λ = 532 nm) Nd:YAG laser. The Nd:YAG laser is capable of producing 600 mJ at 532 nm and has a pulse rate of 10 Hz with a 9 nsec duration, effectively freezing the flow. A Princeton Instruments 14-bit intensified CCD camera, synchronized with the laser, was used to record the images, which were then stored on a PC. The optical setup is shown in Fig. 2. The laser beam is directed to the test section using prisms and focused into a laser sheet approximately 0.5 mm thick. The orientation shown in the figure is for cross sectional views. The optics were also set up so that streamwise images could be recorded.

B. Nozzle Design

Six nozzles have been designed, in addition to a circular baseline nozzle, to explore different parameters of lobed mixers on the mixing process. Photographs of these nozzles are shown in Fig. 3. The baseline nozzle was manufactured from thick wall stainless steel tubing with a nominal one inch diameter (OD). The inside surface was machined to produce a wall thickness of 0.75 mm (ID=23.9 mm), which matches the thicknesses of the lobed nozzles. The lobed nozzles were manufactured from stainless steel bar stock by wire EDM, and 0.75 mm was the smallest thickness attainable (A thinner wall may be possible, but would require annealing of the bar stock prior to cutting). The exit area of the baseline nozzle and that of the lobed nozzles are approximately 450 mm^2. The nozzle outlet geometries are constructed of circular arcs connected with straight lines that are directed radially outward. They are designed to have the same exit flow area as the 1 inch (nominal) tube diameter upstream to which they are attached.

The overall lengths of all the nozzles are 152.4 mm. The nozzles are silver soldered onto the stainless steel tube section, and excess solder is filed smooth to the touch, both inside and out. Nozzle 1 (N1) has inward and outward ramp angles of 10°. Nozzle 2 has the same cross section as N1 but has a ramp angle of 0°. The straight, yet convoluted, section is used to damp out the streamwise vorticity (the circulation of the streamwise vorticity scales with ramp angle, Eqn. 2). Comparing N2 with the baseline nozzle, the effect of increased interfacial contact area can be separated, since the exit perimeter is much greater for N2. Comparing N1 to N2, the effect of adding streamwise vorticity to the flow can be quantified, since the interfacial contact area is the same for both. Nozzle 3, with ramp angles of 20°, is designed to produce the highest level of streamwise vorticity for the nozzles tested.

Figure 4 shows the three four-lobed nozzles tested. All have ramp angles of 10°. Nozzle 4 has the same outlet cross sectional area as the three previous nozzles. The differences are that this nozzle has four lobes, and the perimeter is approximately 30% less. Nozzle 5 is also four lobed, but the lobes have the same geometric shape as the six lobed nozzles. Therefore the cross sectional area is lower. The perimeter is only 4% less than the previous four lobed nozzle. The last nozzle, N6, is a four-lobed mixer with square shaped lobes. This shape was tested to determine whether the corners on the lobes produce other secondary flows that may affect mixing. The geometric parameters of the nozzle are summarized in Table 3.1. Each nozzle was tested under five different flow conditions, summarized in Table 2. Only three of these conditions are reported here: the 30:10 m/sec, 30:30 m/sec, and 30:90 m/sec (inner:outer) flow conditions. The results of the tests for the flow conditions of 90:30 and 90:90 m/sec were similar to 30:10 and 30:30 m/sec, respectively.

Flow visualization for a prototype test nozzle in the present investigation showed a high degree of flow separation for a nozzle with an outward ramp angle of 20° and an inward ramp angle of 10°, which produced a moderate 15% area increase over its 1.25 inch length. Therefore, the nozzles used in the present investigation (except Nozzle 5) were designed to maintain constant cross-sectional area.

III. RESULTS AND DISCUSSION

Figure 5 displays cross sectional averages of fifty instantaneous images taken at three different downstream locations for the baseline and the six-lobed nozzles at a velocity ratio of 3:1 (inner:outer). In this and the following two figures, the nozzles are arranged in order of increasing streamwise vorticity, from top to bottom. D is the diameter of the baseline nozzle (approximately 1 inch). The baseline nozzle shows the expected spreading of the jet downstream. The lobed nozzles indicate similar behavior, but at a higher rate. Nozzle 2, at x/D=1, shows six distinct lobes. By x/D=2, the individual lobes are still distinct, however they have each grown thicker, in addition to growing radially outward. By x/D=3, only the tips of the lobes are noticeable, since adjacent lobes have merged. The spread of the jet of nozzle 2 is greater than the round jet.

Nozzle 1 (10° ramp angle), in Fig. 5, exhibits similar behavior to nozzle 2, but the spread of the smoke has improved due to the addition of streamwise vorticity. For nozzle 3, the changes are even more dramatic. Not only do the individual lobes spread more rapidly, but the entire jet also spreads radially as well. Increasing the lobe angle, thus increasing the strength of streamwise vortices, clearly increases the jet spread. At x/D=1, even these averaged images indicate the existence of counter-rotating streamwise vortices in the form of mushroom-shaped smoke concentrations toward the tip of each lobe for Nozzle 1 and especially Nozzle 3. This shows that the flow is fairly spatially stationary.

Images taken at the nozzle exit fully mapped the exit cross sections of the nozzles and thus showed no evidence of flow separation, so they will not be shown here. Images at x/D locations further downstream (e.g., x/D=5 and 7) show a more mixed cross section, so they will not be presented either.

Similar data are presented in Fig. 6, except that the velocity ratio is now 1:1, i.e., 30 m/sec for both inner and outer streams. This flow condition minimizes the Kelvin-Helmholtz instability but cannot eliminate it completely because of the inner and outer boundary layers at the lobe peaks and non-parallelism of the flow due to the ramps. Nevertheless, the figures show that interface rollup is essentially eliminated. In all cases, the smoke from the individual lobes has not yet merged, and thus the spread of the jet has been significantly reduced . There is still growth of the lobes and overall jet growth but no lobe interaction. With the Kelvin-Helmholtz rollup minimized, the visualizations of the jet issuing from Nozzle 1 and especially Nozzle 3 clearly indicate the existence of streamwise vortices. At x/D=1, the smoke begins to concentrate in the outer tips of the lobes, and at x/D=2, it is turning radially inward towards the centerline. The clearly identifiable, smoke-filled, U-shaped regions at each lobe tip are indicative of two counter-rotating streamwise vortex pairs. The smoke at x/D=3 has diffused even more, especially at the lobe tips. This could be due to the small Kelvin-Helmholtz effect at the lobe tips mentioned earlier and also to the pumping action of the streamwise vorticity.

The results for the last velocity ratio of 1:3 (30:90 m/sec, inner:outer) are presented in Fig. 7. Looking at the figure from left to right, it appears that overall jet spread is small for a given nozzle at various downstream locations, and even less than for the 1:1 velocity ratio. The effect of adding streamwise vorticity is more apparent in terms of spreading of the individual lobes. However, this spreading does not appear to be enough to increase the overall jet spread. The instability characteristics of this case are quite different from the 3:1 case. In Figure 8, RMS images for the baseline nozzle and nozzles 2 and 3, for all three velocity ratios, are shown for one location downstream (x/D=3). The root-mean-square (RMS) intensity fluctuations is high (i.e., brighter) where the fluctuation in intensity (or smoke concentration) is high. A low RMS (i.e. darker regions) could indicate areas where the smoke is well-mixed or areas where there is no smoke at all. The average images in the previous figures should be taken into account when interpreting this data. In any case, the regions of high RMS fluctuations can be used to roughly define the intermittent mixing region. Using this definition, for the circular nozzle, that the mixing region forms a ring shape, as expected. For the velocity ratio of 3:1, the ring structure is well defined, with the inside of the ring being relatively dark. At the velocity ratio of 1:1, the mixing layer is also well defined but occupies a much smaller area and is thinner. The final velocity ratio of 1:3 is similar to the others but shows that there is much more intermittency in the center part of the jet. The 'main' mixing layer (i.e., ring) is slightly thicker than for the 1:1 case. Similar results can be seen for nozzle 2, i.e., the mixing layer for the 1:3 case is thicker than for the 1:1 case but comparable to the 3:1 case. However, the overall spread of the jet for the 3:1 case is higher than the two other cases.

For nozzle 3, the mixing layer does not form a continuous boundary around the nozzle for a velocity ratio of 1:1. There is a small dark spot in the center of the image that indicates very low intermittency. This indicates a very strong jet of smoke issuing from the centerline of the nozzle. Surrounding this dark spot is a ring of high intermittency at the location where the outer, unseeded flow is brought radially inward along the 20° inward ramp. Outside this ring is a dark ring of low mixing that matches the dark section of the average image (Fig. 6). In this region. the smoke has been forced radially outward, and the unseeded air is caught up in the counterrotating vortex pairs, which effectively dilutes the smoke in this region. The outer, lobe-shaped mixing region encompasses the smoke-filled streamwise vortices shown in Fig. 6. The image for the 1:3 velocity ratio once again shows a continuous mixing layer surrounding the central flow and also shows more activity in the interior. The Kelvin-Helmholtz effect is more pronounced and smooth over the structures caused by the streamwise vorticity.

Figures 9 and 10 present streamwise views of instantaneous, average, and RMS images for the baseline nozzle and nozzle 3, respectively. The average and RMS images were calculated using 75 instantaneous images. The laser sheet was vertical and passed through the centerline of the nozzle axis aligned with the lobe tips. The flow is shown moving from left to right from approximately x/D=0 to 8. The drop in intensity at the far right of the images is due to the Gaussian nature of the laser sheet. In Fig.9, at a 3:1 velocity ratio, the jet spreads radially, and the structures are angled upstream. At 1:1, the structures near the nozzle exit are smaller with a slight angle upstream. There appears to be a helical mode developing between x/D of 4 and 6. For the case where the outer flow is faster, a definite downstream angle to the

structures can be seen, as expected. The average images show the relative spreading rates between the different velocity ratios. The spreading of the jet for the 1:3 velocity ratio begins similarly to the 1:1 case, but appears to be slightly higher further downstream. The RMS images show the same general trends. The 3:1 velocity ratio case has an outwardly growing mixing layer, while the case with negligible Kelvin-Helmholtz rollup has very minor spread. On the other hand, the last case shows an inwardly growing mixing layer that eventually merges along the jet centerline, such that the potential core of the jet appears to end at approximately x/D=6.

The three RMS images display flow patterns similar to those has been observed in previous coaxial jet studies by Champagne and Wygnanski,[29] Dahm et al.,[30] and Ko and Au[31]. Champagne and Wygnanski[29] showed that the length of the inner potential core decreased as the inner to outer velocity ratio decreased. Figure 9 clearly shows that the 1:3 velocity ratio case has the shortest potential core length, as evidenced by the intermittent region filling the jet's central region by x/D=6. This behavior was also seen in flow visualizations of low speed water jets by Dahm et al.[30] Other measurements taken by Champagne and Wygnanski[29] and by Ko and Au[31] show that the outer potential core (annular region) is longer than the inner core and that this length is independent of velocity ratio for $U_i/U_o < 1$. The development of the mixing layers in coaxial jets is a complex process. Dahm et al.,[30] suggest that it is an intricate combination of shear layer and wake instabilities that are strongly coupled between inner and outer layers.

Figure 10 presents similar results for nozzle 3 (20° ramp angle). The 3:1 velocity ratio case shows a significant spread relative to the baseline nozzle. The smoke is spreading at approximately the ramp angle, showing that the flow is following the nozzle contour. The average images for the 1:1 and 1:3 ratio cases show a sudden jump in jet growth rate across this plane at approximately x/D=3 which is not noticeable in the instantaneous images. This jump could be indicative of a different instability characteristic. Another possible explanation is that, because the lobed mixer acts as a fluid stirrer until the vortices break down (Eckerle et al.,[22] Werle et al.[15]) and the smaller scale, higher intensity mixing takes place, this break-down is producing the jump in jet spread. The interaction of the outer jet with the quiescent ambient air may also be partially responsible for this behavior. This issue requires further study.

Figure 11 compares streamwise average images for nozzles 1, 2, and 3 at the three velocity ratios. Again, the flow is shown moving left to right from approximately x/D=0 to 8. The 3:1 velocity ratio case shows a higher jet spread with increasing streamwise vorticity. At a 1:1 ratio, there is little interaction between the smoke from the lobes and that exiting along the centerline of the nozzle, as evidenced by the black streaks separating the smoke filled regions. This effect is not as prominent for nozzle 2 because the lobes of the straight section fill completely with smoke and the smoke does not get diluted by inwardly-rushing, unseeded air, thus creating the dark streaks for the other nozzles. When the velocity ratio is other than 1:1, the unmixed (black) streaks are thoroughly mixed by x/D=4. These images also show a sudden jump in jet spread for nozzle 1 that is similar to the spread for nozzle 3.

To quantify the gross mixing of the inner jet with the outer jet, an estimate of the spread of the inner jet (smoke-marked area) was made. Every pixel intensity above a certain threshold was counted as part of the spreaded center jet, and those below the threshold were considered background. Plotting a histogram of the number of pixels vs pixel intensity for the average images was found to provide an adequate method for separating pixels representing smoke from pixels representing background intensity. For the majority of the images, the 'signal' was readily apparent, forming a 'hump' in the data at the higher end of the intensity scale. The other images (usually at the higher x/D values) did not have a readily discernible hump in the histogram. These images exhibited a relatively flat portion followed by a dropoff at the higher intensities. Results are shown in Fig. 12. In this figure, the calculated area of the spreaded inner jet normalized by the exit area of the baseline jet is plotted versus x/D location for four different nozzles. The total image size is 288x192 (=55296) pixels, while the nozzle exit area is approximately 1100 pixels. The graphs show a general trend of increasing spreaded inner jet area with increasing distance downstream and also with increasing streamwise vorticity. Figure 12a shows that the inner jet from nozzle 3 grows to approximately thirty times its original size. While these graphs corroborate the trends in the images previously shown, these inner jet spread region estimates should be considered nominal estimates, particularly at the furthest downstream locations.

One of the objectives of the present study is to separate the contributions to overall mixing due to the increase in interfacial area and the streamwise vorticity generated by the lobed nozzles. The difference in the spreaded inner jet area between nozzle 2 (0° ramp) and the baseline nozzle provides the contribution to total mixing due to the increase in interfacial area. The difference in the spreaded inner jet area between nozzle 1 (10° ramp) and the baseline nozzle provides the contribution to mixing due to both interfacial area and streamwise vorticity. The contribution due to streamwise vorticity alone is found by subtracting the two. Using the data of Fig. 12, these separate effects on mixing enhancement can be found and their relative contributions calculated. Table 3 shows the results for several x/D locations for nozzle 1. The x/D locations of 5 and 7 are not shown because the spreaded inner jet area calculations for these locations have the most uncertainty due to some clipping of the images by the laser sheet. At x/D=1 and a velocity ratio of 3:1, the contribution to overall mixing due to streamwise vorticity is greater than the contribution of the interfacial area. Moving downstream, the contribution from the interfacial area decreases slightly, while the streamwise vorticity enhancement increases. This is consistent with previous work (Werle et al.,[15] Eckerle et al.[22]) showing that the streamwise vortices grow first, then break down downstream, thereby increasing turbulence levels and mixing. As the vortices go through the processes of stretching, pairing, and tearing, mixing increases. For the velocity ratio of 1:1, the interfacial area provides a much larger fraction of the mixing than the streamwise vorticity at x/D=1. The same trends as for the 3:1 velocity ratio are evident moving downstream. However, the fractional contribution due to interfacial area decreases--hence, that due to streamwise vorticity increases--at a much faster rate. Since the Kelvin-Helmholtz effect is minimized for this case, the streamwise vortices are the dominant structures in the flow. As they interact downstream, their mixing effects are more prevalent. The results for the 1:3 velocity ratio are similar to the previous two cases. The

relative contributions to mixing at x/D=1 are in approximately the same proportions as for the 1:1 case, but the change in proportions moving downstream is about the same as the 3:1 case.

Figure 13 shows the data of Fig.12 and Table 3, for the different velocity ratios. The bar graphs show the total mixing for nozzle 1 at three different locations downstream, but with the interfacial area and streamwise vorticity contributions shaded differently. Even though the fraction of mixing due to the interfacial area decreases as velocity ratio increases, the total amount of mixing due to interfacial area is still significant, contributing at least 30% to the total mixing in all cases. Comparing different velocity ratios for each x/D location, there is a distinct increase in total mixing as velocity ratio increases and the percentage of enhancement due to streamwise vorticity increases. This is in agreement with Manning's results, except Manning did not discuss any effect due to downstream distance.

Selected results for the three four-lobed nozzles are shown in Fig. 14. The 1:1 velocity ratio case was chosen because the evolution of the streamwise vorticity is more easily seen. In general, the same trends were observed in the four-lobed nozzles as for the six-lobed ones. Figure 14 shows the differing levels of streamwise vorticity developed at all three velocity ratios and several distances downstream. The larger lobes of nozzle 4 produce slightly larger counter-rotating vortex pairs than the smaller lobes of nozzle 5. The counter-rotating vortex pairs generated in nozzle 6 are, to some degree, masked by small scale structures generated at the corners.

IV. SUMMARY

Flow visualizations using a passive scalar have been performed to explore mixing enhancement in an axisymmetric coaxial jet with an inner lobed mixer. Seven different central jet geometries, six lobed-mixer nozzles and a circular nozzle, were used to investigate three different mixing mechanisms involved, namely the increased interfacial contact area, the streamwise vorticity, and the inner/outer velocity ratio. Instantaneous and average images showed the pronounced effect of the Kelvin-Helmholtz rollup on mixing even with the presence of very strong streamwise vortices. The fraction of mixing enhancement due to streamwise vorticity (relative to mixing enhancement due to increased interfacial contact area) was found to increase as velocity ratio increased. In addition, this fraction increased with downstream distance. Overall, the lobed mixer nozzle with the largest ramp angle of 20° (strongest streamwise vortices) , produced the highest mixing at all velocity ratios.

REFERENCES

[1]Paterson, R.W., [1982], "Turbofan Forced Mixer-Nozzle Internal Flowfield," NASA Contractor Report 3492.

[2]Paterson, R.W., [1984], "Turbofan Mixer Nozzle Flow Field--A Benchmark Experimental Study," ASME J of Engineering for Gas Turbines and Power, Vol.106, pp.692-698.

[3]Povinelli, L.A., B.H. Anderson, and W. Gerstenmaier, [1980], "Computation of Three Dimensional Flow in Turbofan Mixers and Comparison with Experimental Data," AIAA Paper 80-0227.

[4]Frost, T.H., [1966], "Practical Bypass Mixing Systems for Fan Jet Aero Engines," Aeronautical Quarterly, v.17, pp.141-161.

[5]Anderson, B., Povinelli, L., and W. Gerstenmaier, [1980], "Influence of Pressure Driven Secondary Flows on the Behavior of Turbofan Forced Mixers," AIAA Paper 80-1198.

[6]Birch, S.F., G.C. Paynter, D.B. Spalding and D.G. Tatchell, [1977],"An Experimental and Numerical Study of the 3-D Mixing Flows of A Turbofan Engine Exhaust System," AIAA Paper 77-0204.

[7]Blackmore, W.L. and C.E. Thompson, [1981], "3-D Viscous Analysis of Ducts and Flow Splitters," AIAA Paper 81-277.

[8]Crouch, R.W., Coughlin, C.L., and G.C. Paynter, [1976], "Nozzle Exit Flow Profile Shaping for Jet Noise Reduction," AIAA Paper 76-511.

[9]Head, V.L., L.A. Povinelli, and W.H. Gerstenmaier, [1984], "Hot-Flow Tests of a Series of 10-Percent Scale Turbofan Forced Mixing Nozzles," NASA Technical Paper No. 2268.

[10]Kozlowski, H. and G. Kraft, [1980], "Experimental Evaluation of Exhaust Mixers for an Energy Efficient Engine," AIAA Paper 80-1088.

[11]Kuchar, A.P. and R. Chamberlin, [1980], "Scale Model Performance Test Investigation of Exhaust System Mixers for an Energy Efficient Engine (E^3) Propulsion System," AIAA Paper 80-229.

[12]Shumpert, P.K., [1980], "An Experimental Model Investigation of Turbofan Engine Internal Exhaust Gas Mixer Configurations," AIAA Paper 80-228.

[13]Packman, A.B., Kozlowski, H. and O. Gutierrez, [1976], "Jet Noise Characteristics of Unsuppressed Duct Burning Turbofan Exhaust Systems," AIAA Paper 76-149.

[14]Povinelli, L.A. and B.H. Anderson, (1984), "Investigation of Mixing in a Turbofan Exhaust Duct, Part II: Computer Code Application and Verification," AIAA Journal, Vol.22, No.4, pp.518-525.

[15]Werle, M.J., Paterson, R.W. and W.M. Presz, Jr., [1987], "Flow Structure in a Periodic Axial Vortex Array," AIAA Paper 87-610.

[16]Presz, W. Jr., Gousy, R. and B. Morin, [1986], "Forced Mixer Lobes in Ejector Designs," AIAA Paper 86-1614.

[17]Skebe, S.A., McCormick, D.C. and W.M. Presz, Jr., [1988], "Parameter Effects on Mixer-Ejector Pumping Performance," AIAA Paper 88-188.

[18]Malecki, R., S. Mityas, and W. Lord, (1990), "Navier-Stokes Analysis of an Ejector and Mixer-Ejector Operating at Pressure Ratios in the Range 2-4," AIAA Paper 90-2730.

[19]Tillman, T.G., Patrick, W.P. and R.W. Paterson, [1988], "Enhanced Mixing of Supersonic Jets" AIAA Paper 88-3002.

[20]McVey J.B., [1988], "Observation of the Effect of Streamwise Vorticity on the Spreading of Flames in High Speed Flow," Combustion Science and Technology, v.60, pp.447-451.

[21]McVey J.B. and J. Kennedy, [1989], "Flame Propagation Enhancement Through Streamwise Vorticity Stirring," AIAA Paper 89-619.

[22]Eckerle, W.A., Sheibani, H. and J. Awad, [1990], "Experimental Measurement of the Vortex Development Downstream of a Lobed Forced Mixer," ASME Paper 90-GT-27.

[23]Barber, T., R.W. Paterson, and S.A. Skebe, [1988], "Turbofan Forced Mixer Lobe Flow Modeling. Part I. Experimental and Analytical Assessment," NASA Contractor Report, CR 4147.

[24]Manning, T.A., [1991], "Experimental Studies of Mixing Flows with Streamwise Vorticity," Masters Thesis, Massachusetts Inst. of Technology.

[25]Elliott, J.K., T.A. Manning, Y.J. Qiu, E.M. Greitzer, C.S. Tan and T.G. Tillman, [1992b], "Computational and Experimental Studies of Flow in Multi-Lobed Forced Mixers," AIAA Paper 92-3568.

[26]McCormick, D.C., [1992], "Vortical and Turbulent Structure of Planar and Lobed Mixer Free-Shear Layers," Ph.D. Dissertation, University of Connecticut.

[27]McCormick, D.C. and Bennett, J.C., Jr, [1993], "Vortical and Turbulent Structure of a Lobed Mixer Free-Shear Layer," AIAA Paper 93-219.

[28]Presz, W.M.Jr., G. Reynolds, and D. McCormick, [1994], "Thrust Augmentation Using Mixer-Ejector-Diffuser Systems," AIAA Paper 94-0020.

[29]Champagne, F.H. and Wygnanski, I.J., (1971), "An Experimental Investigation of Coaxial Turbulent Jets," Intl. Journal of Heat Mass Transfer, Vol.14, pp.1445-1464.

[30]Dahm, W.J.A., C.E. Frieler, and G. Tryggvason, (1992), "Vortex Structure and Dynamics in the Near Field of a Coaxial Jet," J Fluid Mechanics, Vol.241, pp.371-402.

[31]Ko, N.W. and H. Au, (1985), "Coaxial Jets of Different Mean Velocity Ratios," J of Sound and Vibration, Vol.100, No.2, pp.211-232.

Table 1 Nozzle Geometries

Nozzle	Description	Length of nozzle	Ramp Angles	Exit Area	Exit Perimeter
Baseline	circular	NA	NA	448 mm^2	75 mm
1	6 lobes, long	50.8 mm	9.6°/10°	453 mm^2	246 mm
2	6 lobes, straight	76.2 mm	0°/0°	453 mm^2	246 mm
3	6 lobes, short	25.4 mm	19°/20°	453 mm^2	245 mm
4	4 lobes, large	50.8 mm	9.6°/10°	453 mm^2	176 mm
5	4 lobes, small	50.8 mm	9.6°/10°	322 mm^2	169 mm
6	4 lobes, square	50.8 mm	10°/10°	453 mm^2	170 mm

Table 2 Operating Conditions

Operating Condition	V_{inner} [m/sec]	V_{outer} [m/sec]	$V_{pri}:V_{sec}$
1	30	10	3:1
2	30	30	1:1
3	30	90	1:3
4	90	30	3:1
5	90	90	1:1

Table 3 Contributions to Mixing by Interfacial Area and Streamwise Vorticity for Nozzle 1

Velocity Ratio	Contribution of:	x/D = 1	x/D = 2	x/D = 3
3:1	Interfacial Area Streamwise Vorticity	40% 60%	39% 61%	32% 68%
1:1	Interfacial Area Streamwise Vorticity	73% 27%	58% 42%	37% 63%
1:3	Interfacial Area Streamwise Vorticity	72% 28%	63% 37%	52% 48%

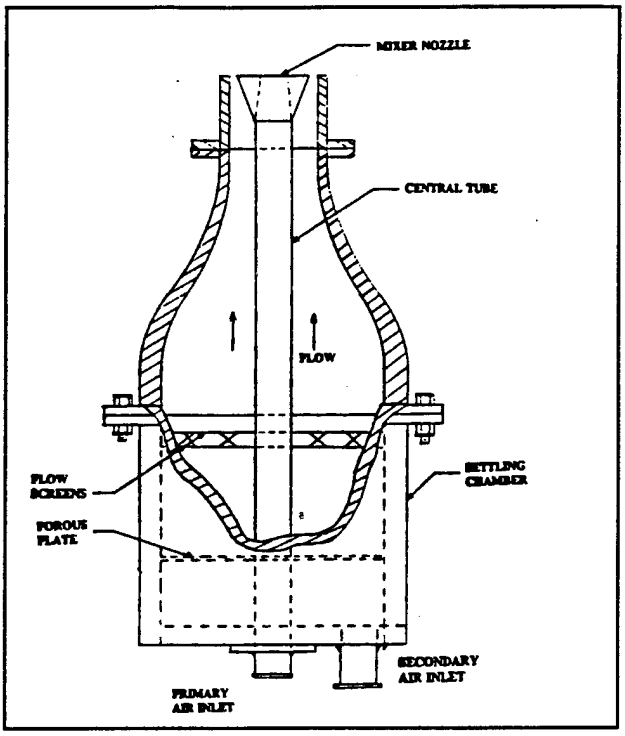

Figure 1. Schematic of settling chamber and contraction section.

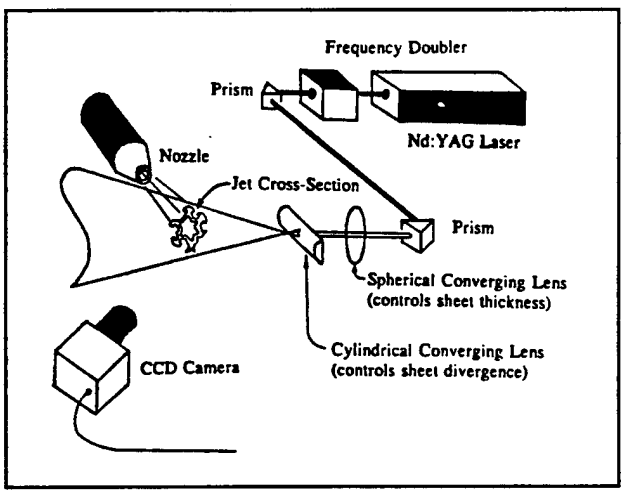

Figure 2. Optical setup for flow visualizations.

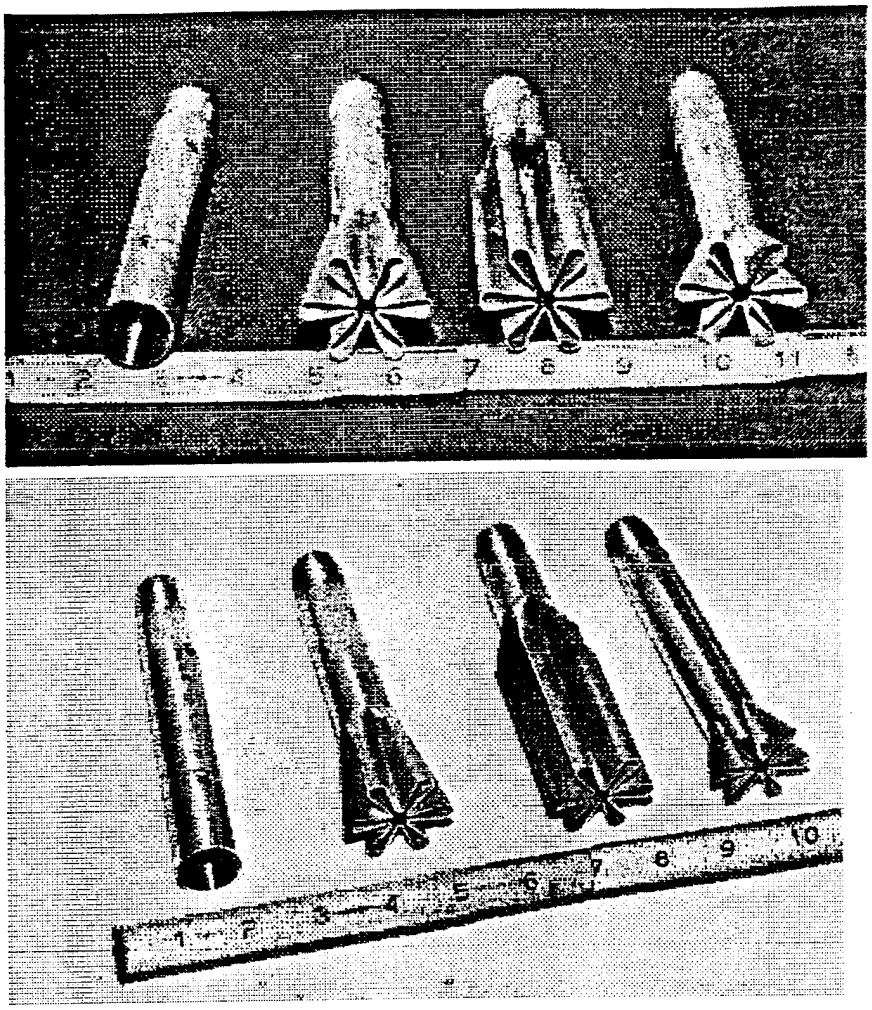

Figure 3. Views of the baseline circular nozzle and 6-lobed nozzles. From left to right they are: baseline circular, nozzle 1 (10 deg.), nozzle 2 (0 deg.), and nozzle 3 (20 deg.).

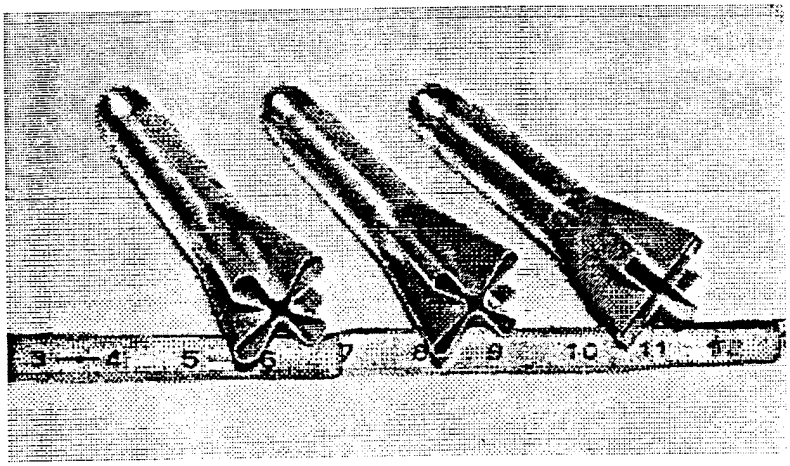

Figure 4. The 4-lobed nozzles are shown from left to right: nozzle 4, 5 and 6.

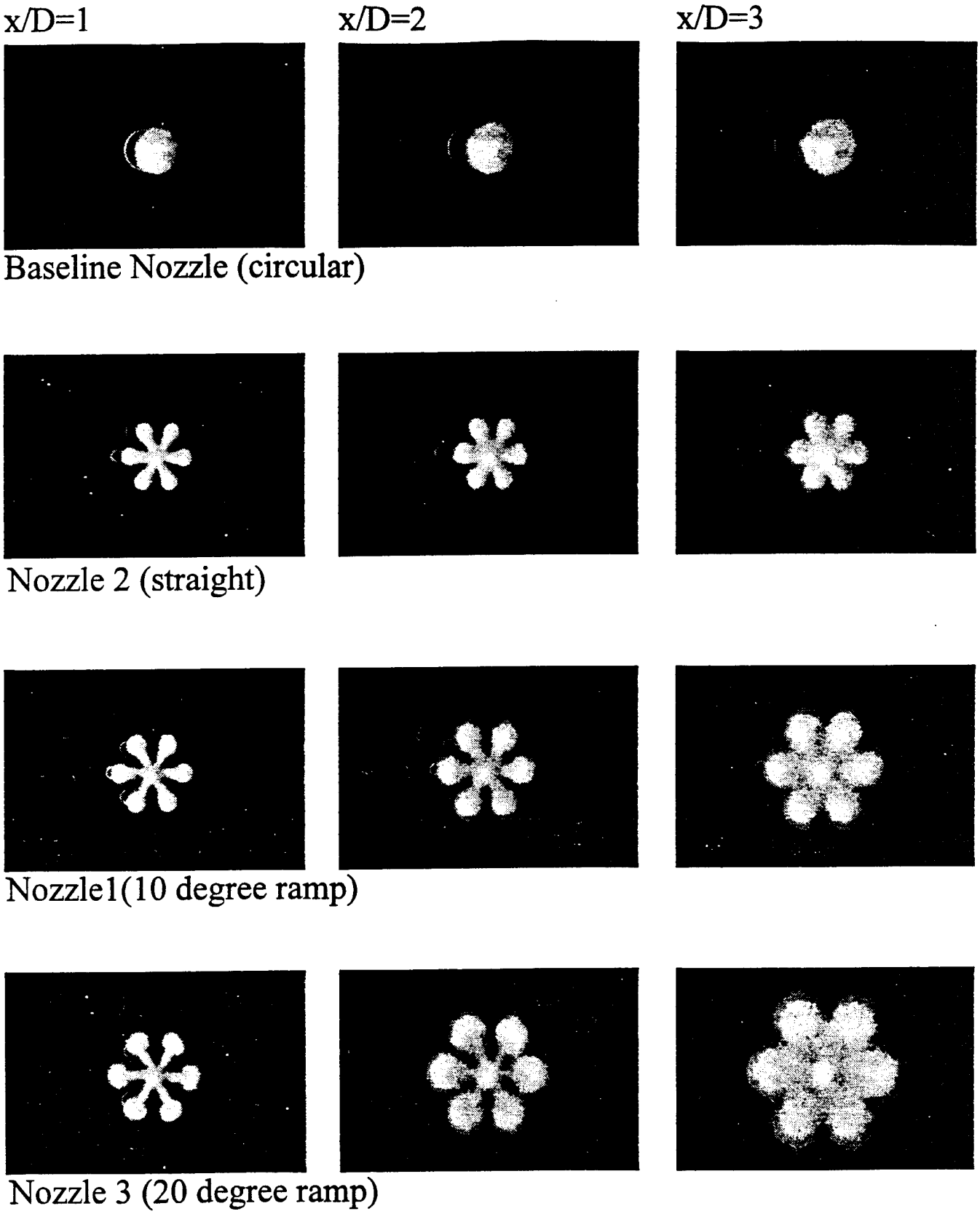

Figure 5. Effect of adding streamwise vorticity for a velocity ratio of 30:10m/sec (inner:outer).

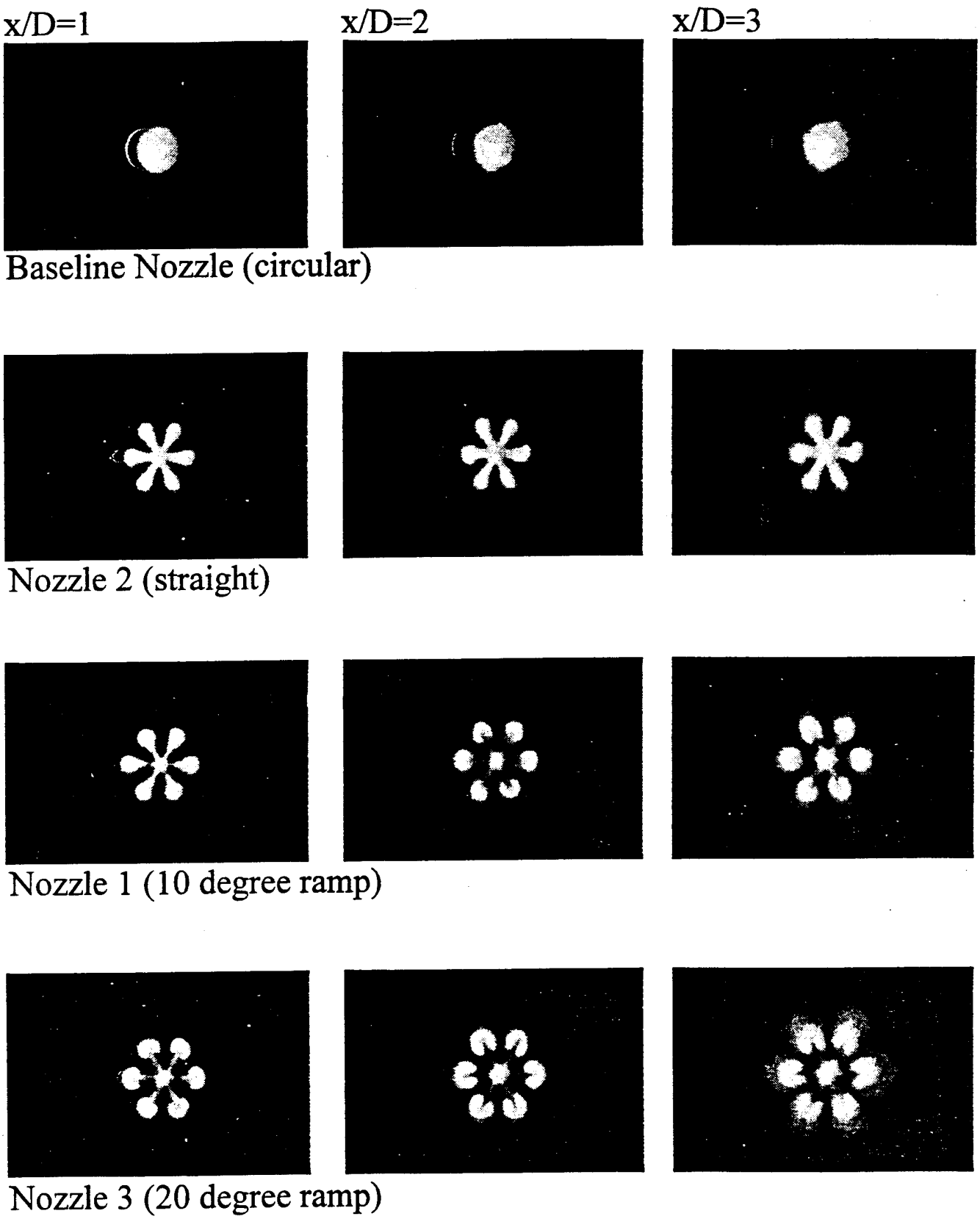

Figure 6. Effect of streamwise vorticity at a velocity ratio of 30:30m/sec (inner:outer).

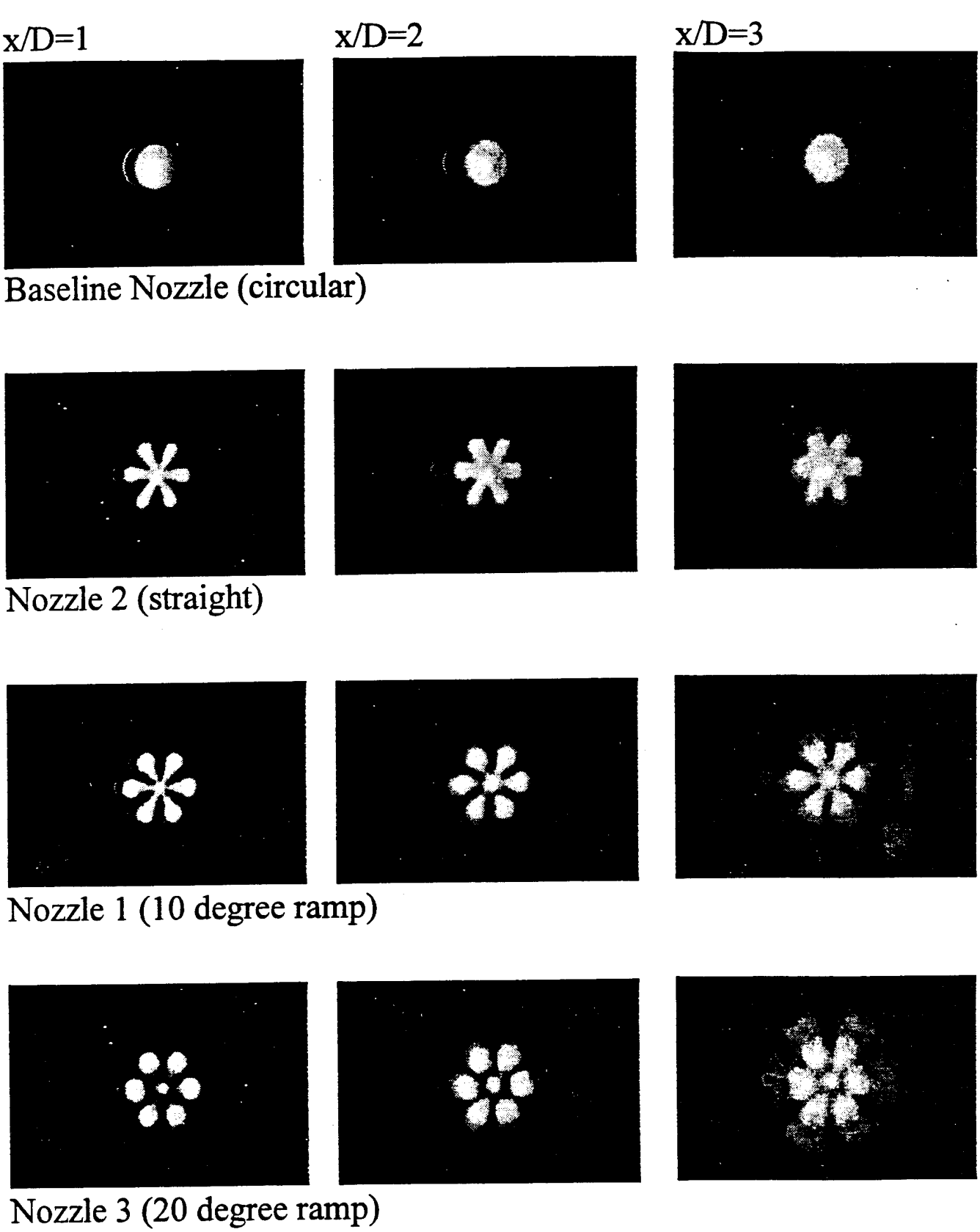

Figure 7. Effect of streamwise vorticity for a velocity ratio of 30:90m/sec (inner:outer).

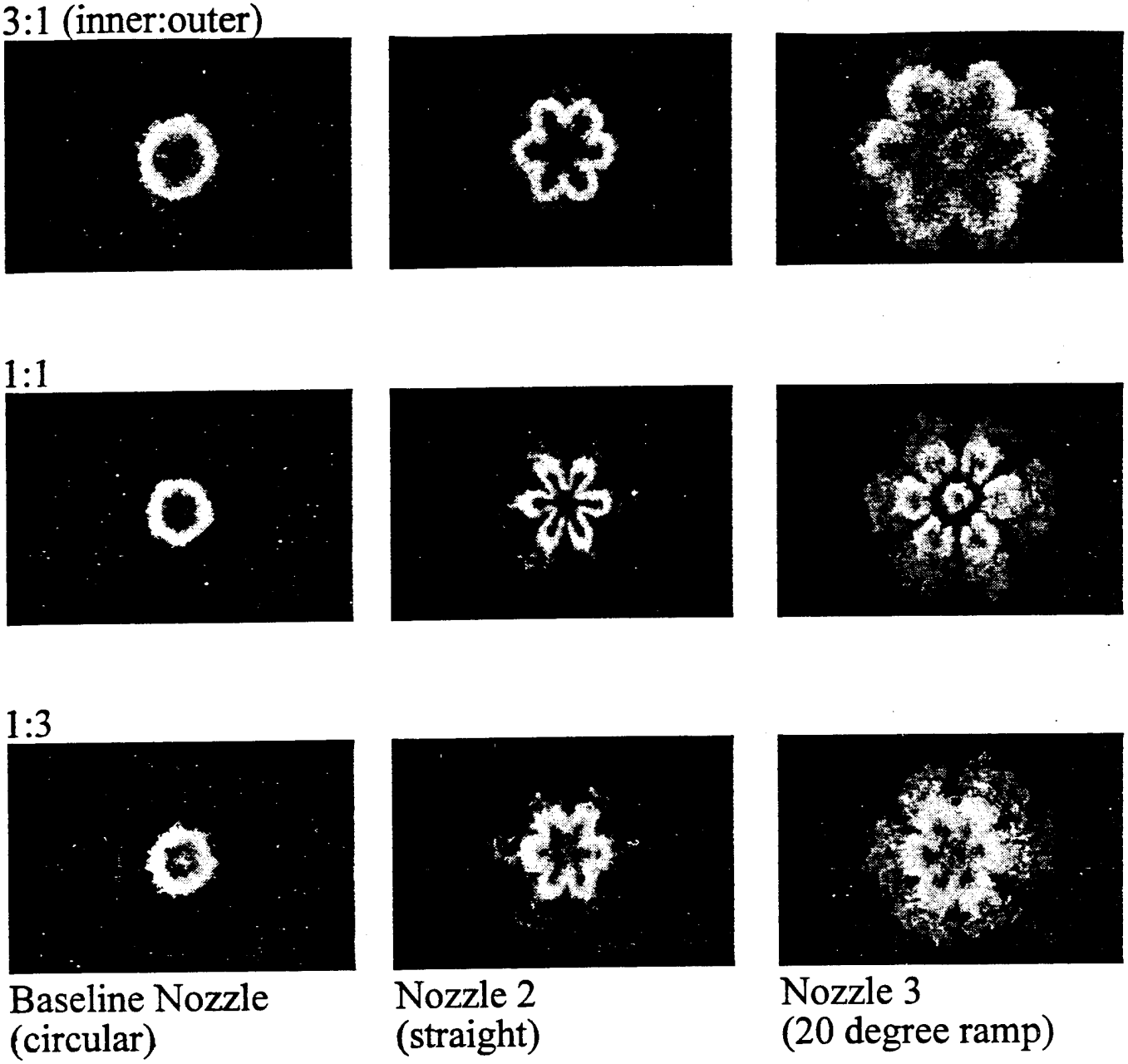

Figure 8. Comparison of RMS images at x/D=3, showing effect of Kelvin-Helmholtz and streamwise vorticity

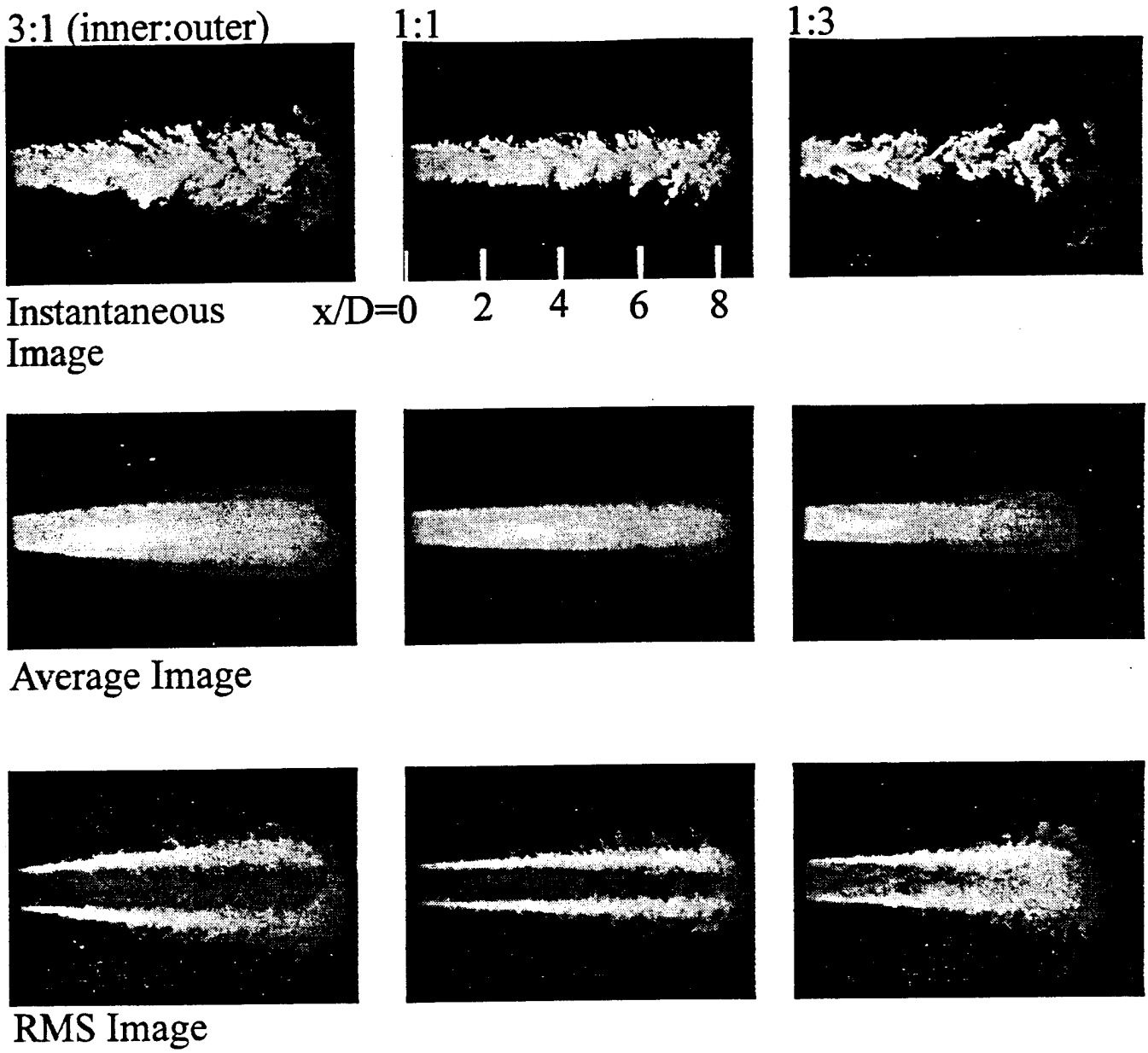

Figure 9. Baseline nozzle comparison of instantaneous, average, and RMS images.

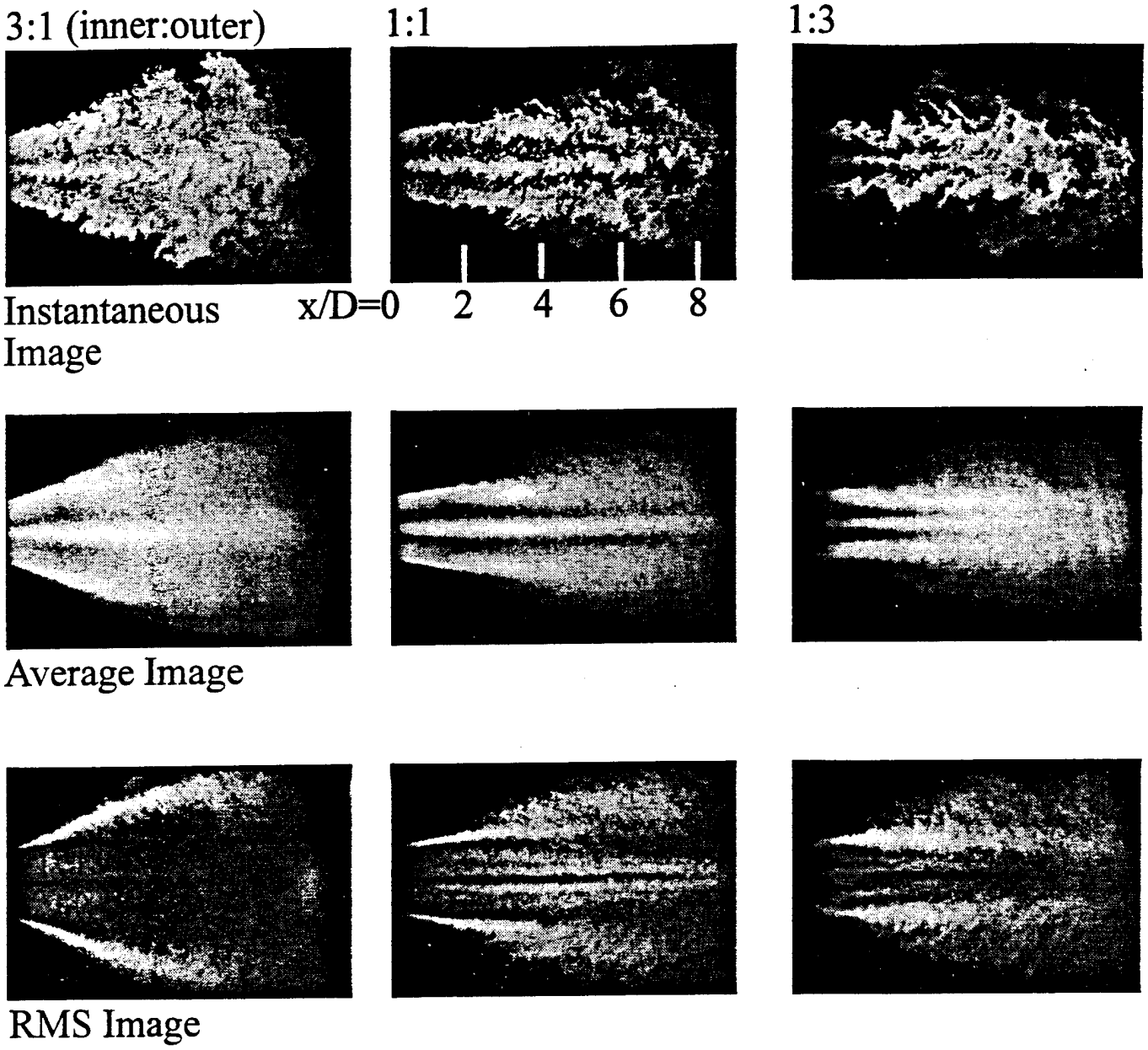

Figure 10. Comparison between instantaneous, average and RMS images for nozzle 3.

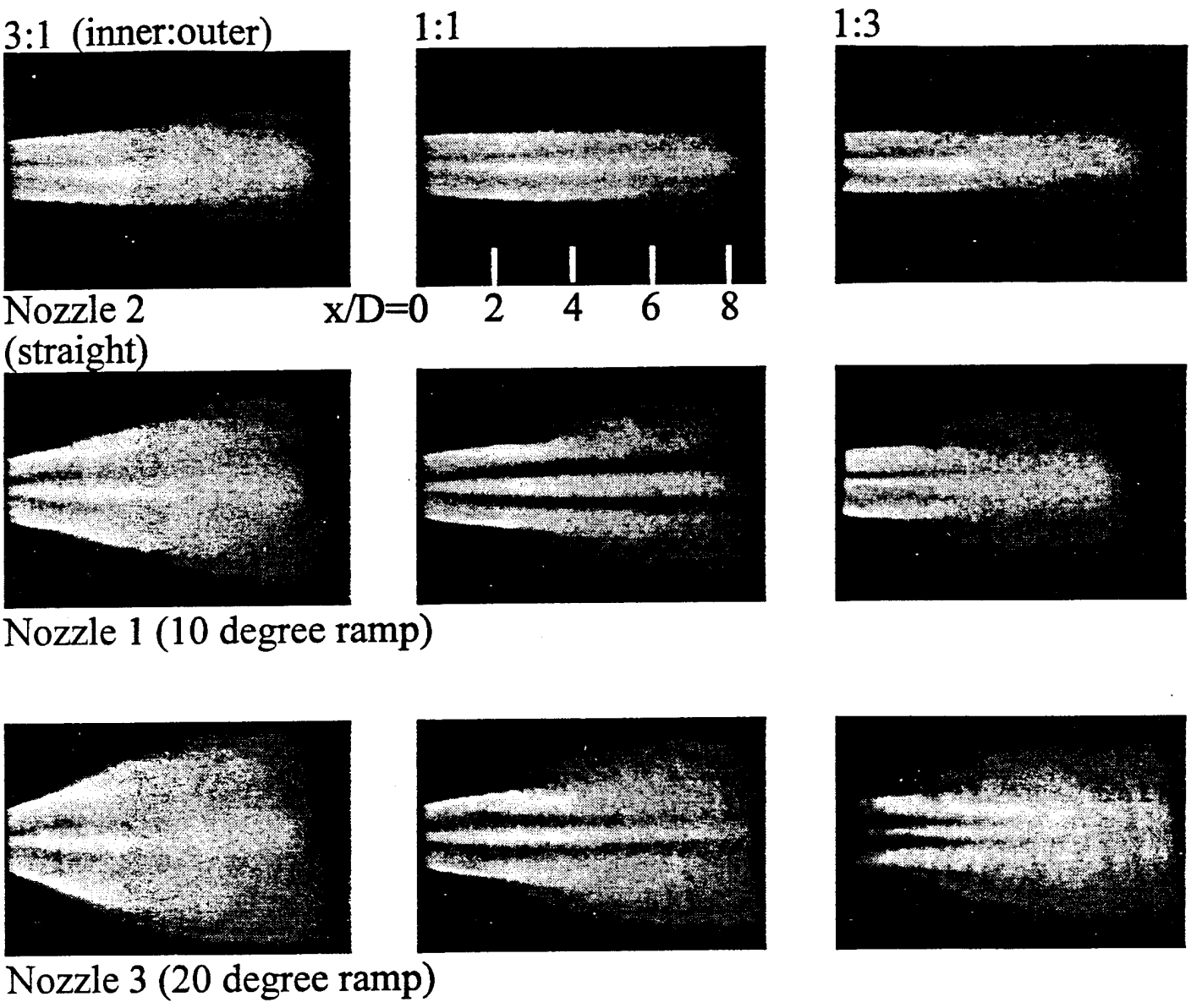

Figure 11. Streamwise views of the three six-lobed nozzles for the three velocity ratios.

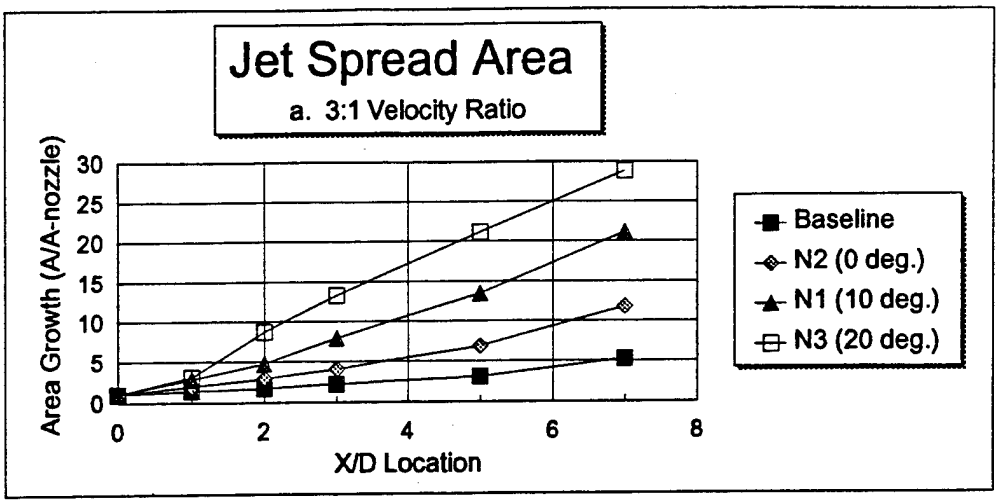

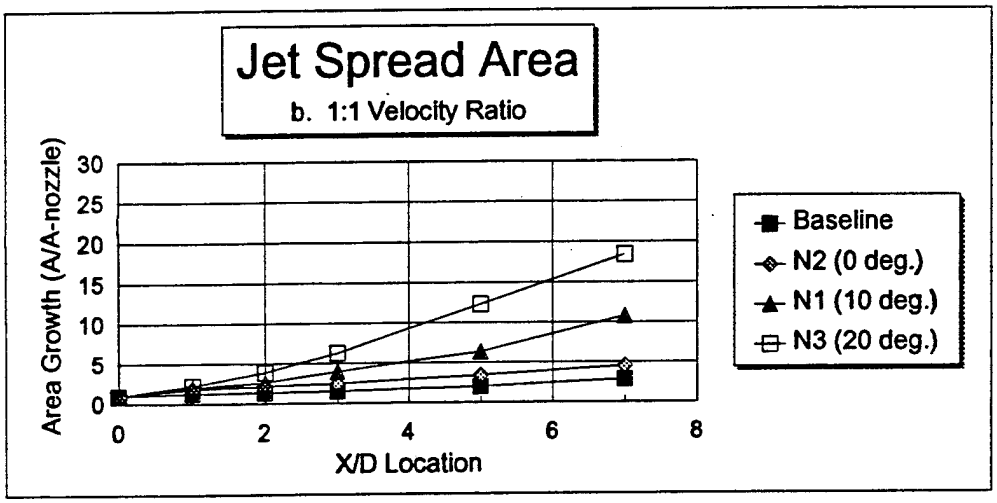

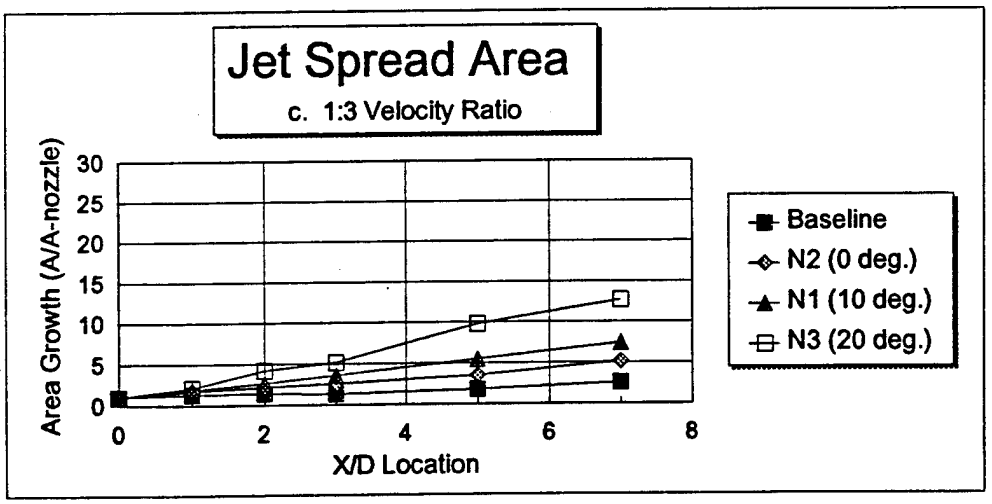

Figure 12. Comparison of jet spread for the six-lobed nozzles.

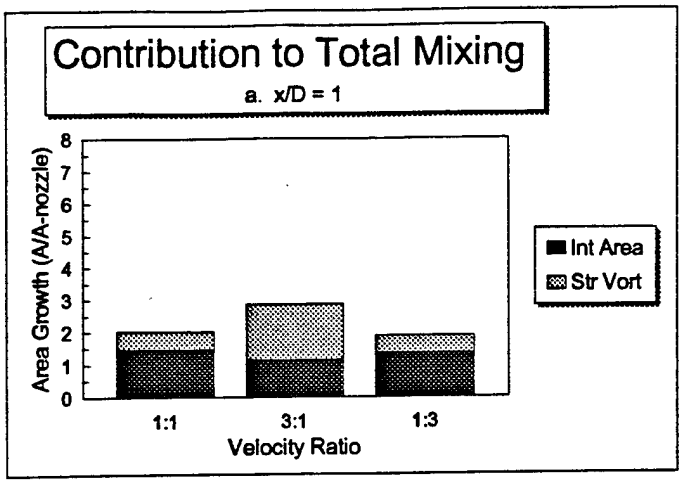

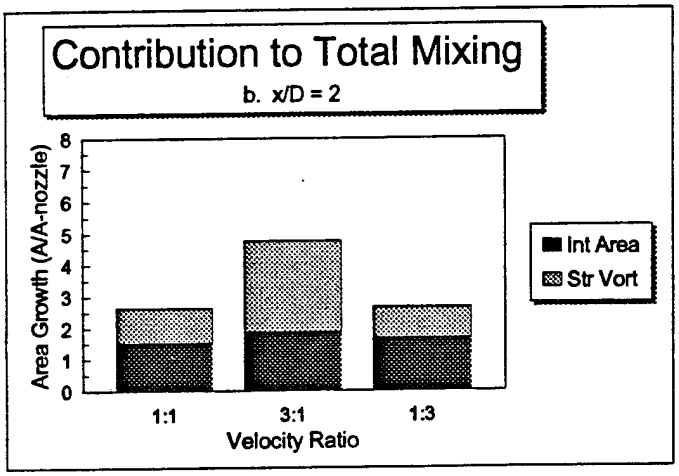

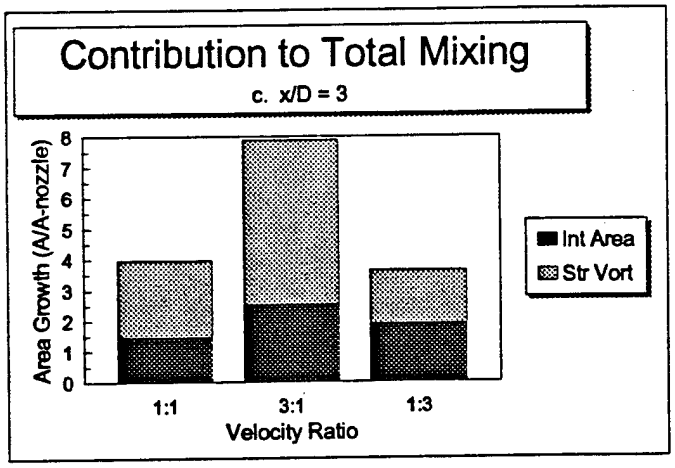

Figure 13. Comparison of absolute contributions of interfacial contact area and streamwise vorticity to total mixing for the 10 degree ramp angle nozzle.

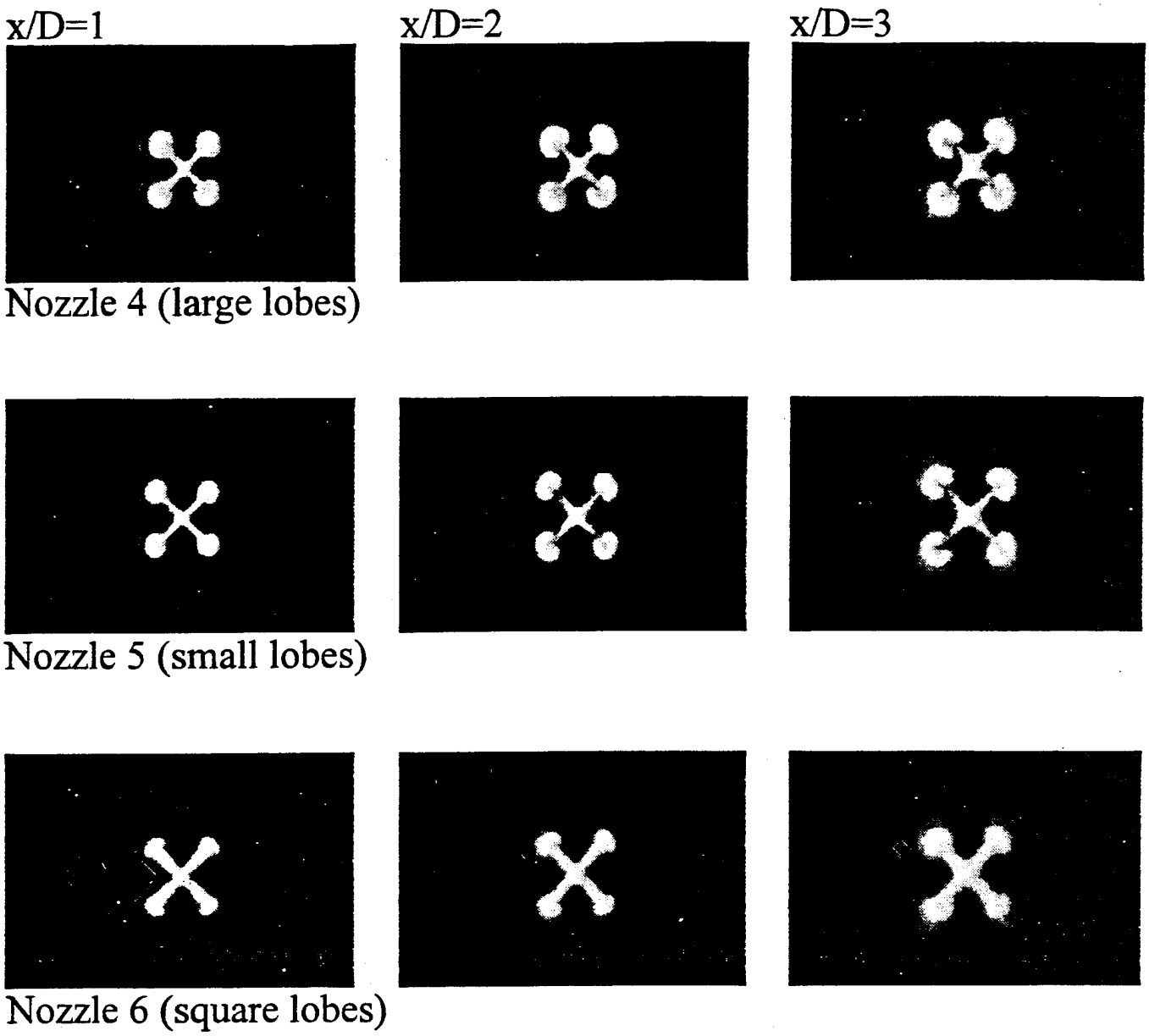

Figure 14. Streamwise vorticity generation in the four-lobed nozzles at a 1:1 velocity ratio (average images).